Int. J. Cancer: **117,** 387–397 (2005)

Adenoviral modulation of the tumor-associated system L amino acid transporter, LAT1, alters amino acid transport, cell growth and 4F2/CD98 expression with cell-type specific effects in cultured hepatic cells

Bill T. Storey[2], Celine Fugere[1], Anne Lesieur-Brooks[1], Charles Vaslet[2] and Nancy L. Thompson[1,2]*

[1]*Department of Medicine, Division of Hematology and Medical Oncology, Rhode Island Hospital, Providence RI, USA*
[2]*Department of Pathology and Laboratory Medicine, Brown University, Providence, RI, USA*

Altered expression of metabolite transporters is observed frequently in tumor cell lines and primary neoplasms. The extent to which these may to contribute to the growth autonomy associated with cancer is not clear. LAT1 is a major L-type amino acid transporter over-expressed in a variety of cancer types and a light chain component of the CD98 heterodimer. We utilized an adenoviral expression system to modulate the level of LAT1 in a hepatic *in vitro* model to examine phenotypic changes associated with short-term exogenous and blocked expression. LAT1 levels were increased three fold and resulted in increased L-type amino acid transport as a result of adenoviral expression in murine hepatocytes. The protein was expressed on the cell surface and complexed with the CD98 heavy chain known as 4F2. Surprisingly, levels of the total CD98 protein complex were increased 2.4-fold as a result of adenoviral expression of light chain only, suggesting coordinate regulation. Exogenous overexpression was less effective in normal rat liver cells relative to mouse. LAT1 antisense expression in hepatic tumor cells resulted in a modest though statistically significant decrease in cell number, viability and S-phase cells over a 5-day period relative to controls despite the absence of a significant decrease in L-type transport over this period. These studies are preparatory to *in vivo* efforts focusing on LAT1/CD98 as a potential therapeutic target.
© *2005 Wiley-Liss, Inc.*

Key words: LAT1; 4F2; CD98; leucine; adenovirus

Recent studies have demonstrated that LAT1 is a major L-type amino acid transporter in a variety of cancer cells including hepatic,[1–3] oral,[4] breast,[5] bladder[6] and colon.[7] This predicted 12 transmembrane spanning protein mediates sodium independent transport of large neutral amino acids including several essential amino acids and is a major route for providing tumor cells with branched and aromatic amino acids. Because these amino acids are indispensable for growth and proliferation-dependent protein synthesis, LAT1 represents a target of high potential therapeutic interest. LAT1 exhibits broad substrate selectivity and is responsible for transport not only of naturally occurring amino acids, but also amino acid-related drugs such as L-dopa, melphalan, (an anti-cancer phenylalanine mustard), triiodothyronine and thyroxine and gabapentin, an anti-convulsant. Functional expression of LAT1 in the plasma membrane requires an additional single transmembrane glycoprotein known as 4F2 antigen or heavy chain and together these form a heterodimeric complex known as CD98.[8–13] The glycoprotein-associated transporters are a novel class of amino acid transporters recently the subject of much interest not only in relation to transport but also to CD98-linked functions in cell activation, integrin signaling, cell fusion and malignant transformation.[14–17]

Our research has utilized a tetracycline-inducible adenoviral expression system (TET-Off) system to alter levels of LAT1 and 4F2 *in vitro*. We have increased LAT1 expression in normal hepatic cells to determine functional changes occurring in processes associated with cancer. We have also utilized an antisense adenoviral construct to decrease LAT1 expression. As the field has progressed, various terms have been used for cationic amino acid transporters and heterodimeric amino acid transporters.[8] We consistently use the terms LAT1 and 4F2 for the light and heavy chains of the CD98 complex in our study although TA1,[7] E16[7] and SLC7A5[8] have been utilized in previous research describing the CD98 light chain and CD98hc and SLC3A2 have also been used to describe the heavy chain.[8]

Despite implications that LAT1 may represent an attractive clinical target for tumor and other pathological forms of cell proliferation, it is not yet known if specific modulation of LAT1, independent of CD98, may impact function. Our current studies were designed to ask whether an inducible adenoviral expression system was effective in driving short term blocked expression and overexpression of LAT1 in an *in vitro* hepatic model and to relate such modulation to functional effects including transport and cell growth. We hypothesize that upregulation of LAT1 provides an adaptive advantage to the tumor cell, particularly under conditions of limiting nutrients. We had reported previously constitutive LAT1 expression associated with neoplastic growth *in vitro* and *in vivo*,[1,7,18,19] In previous work, a significantly greater number of normal murine hepatic cells were able to survive low amino acid conditions over 48 hr after transient exogenous expression of LAT1, independent of exogenous 4F2.[19] We believed that as the primary L-type transporter in tumor cells, LAT1 modulation could thus directly impact tumor cell growth or survival.

We overexpressed LAT1 and 4F2 individually and in combination to assess cellular alterations potentially mediating neoplastic transformation. It has been shown previously that 4F2 overexpression in NIH 3T3 cells results in changes consistent with malignant transformation[17,20] and monoclonal antibodies against 4F2 have been shown to inhibit tumor cell nucleic acid synthesis and proliferation of several cell types.[21,22] The malignant alterations, however, required association with the CD98 complex light chain.[20]

We utilized a tetracycline-inducible adenoviral expression system (TET-Off) to alter levels of LAT1, with the goal of assessing the short-term functional impact on *in vitro* phenotypes important to cell growth and survival. We extended our research from the previously utilized normal, murine hepatocyte cultures (AML12)[19] to a normal rat hepatocyte line (WB) and a well-matched derivative tumor cell line (GP7TB) produced from WB.[18] We demonstrated high level expression in a hepatic *in vitro* model system with a surprising coordinate upregulation of 4F2 protein resulting from exogenous LAT1 expression. Virally driven antisense LAT1 expression in hepatic tumor cells resulted in moderate but significant decreases in cell viability and cells in S-phase. Despite unexplained cell type specific variability in functional outcome, these introductory studies validate the approach of targeting this molecule and serve as preparation for *in vivo* experimentation.

Material and methods

Adenoviral constructs and optimization of adenoviral infection

An Adeno-X TET-Off Cloning System (Clontech, Palo Alto, CA) was used to generate recombinant adenoviral constructs

Grant sponsor: NIH; Grant number: R01CA73611, P20RR017695
***Correspondence to:** Medical Oncology, Rhode Island Hospital, 593 Eddy Street, Providence, RI. Fax: +401-444-8141.
E-mail: Nancy_Thompson@Brown.edu
Received 20 December 2004; Accepted after revision 28 February 2005
DOI 10.1002/ijc.21169
Published online 17 May 2005 in Wiley InterScience (www.interscience.wiley.com).

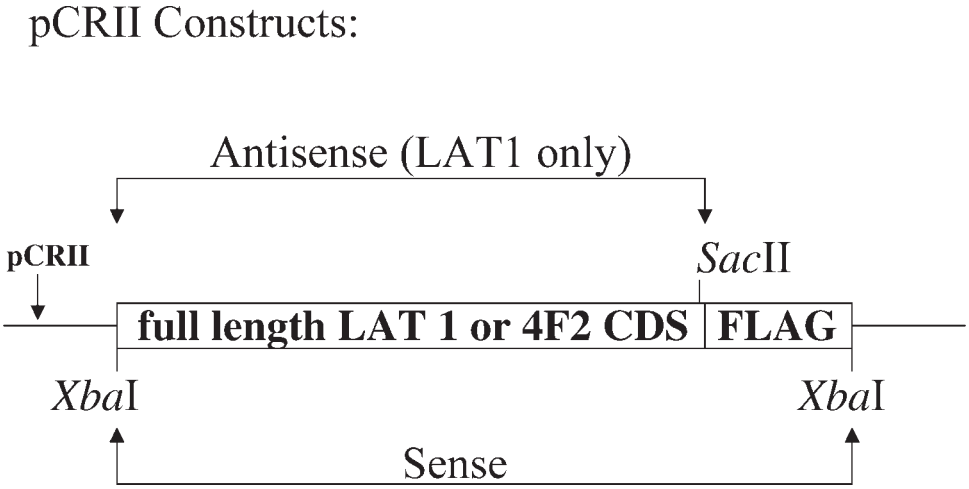

FIGURE 1 – Generation of recombinant adenoviral constructs containing full-length rat LAT1 sense (Genbank accession number AB015432) or antisense coding sequences (CDS) as well as human 4F2 (Genbank accession number AB018010). Sense (*Xba*I-*Xba*I) and antisense (*Xba*I-*Sac*II for LAT1 only) fragments were isolated from these constructs and subcloned into the pTRE-Shuttle 2 vector containing an adenoviral expression cassette.

containing the rat LAT1 sense or antisense sequence as well as the human 4F2 sequence under tetracycline control. The full length LAT1 coding sequence (GenBank accession number AB015432) region was PCR amplified from pFLAG-CMV5a rat LAT1[19] using forward (5′ TCTAGAAAGCTTATGGCGGTCGCGGGCCAAAG 3) and reverse (5′ TCTAGAAAGCTTCTACTTGTCGTCATCGTCTTTGTAGTCGACCGCGGTCTCCTGAGGAACCACCTGC 3) primers. These primers position an in-frame FLAG reporter peptide sequence (DYKDDDDK) immediately downstream of LAT1 and a *Sac*II site (5 C↓CGCGG 3), and also flank the fusion sequence with *Xba*I (5 T↓CTAGA 3) sites. Similarly, the full length 4F2 coding sequence (Genbank accession number AB018010) was PCR amplified from pFneo-4F2[10] using forward (5′ TCTAGAATGAGCCAGGACACCGAGGTGGATATG 3) and reverse (5′ TCTAGATCACTTGTCGTCATCGTCTTTGTAGTCGGATCCGGCCGCGTAGGGGAAGCGGAGCAGCAG 3) primers with an in-frame FLAG sequence and outside *Xba*I sites. These amplicons were cloned into a pCRII-TOPO A/T vector (Invitrogen, Carlsbad, CA) for DNA sequence confirmation (Keck Labs, Yale University) and subsequent restriction (Fig. 1). Full sense (*Xba*I-*Xba*I) and antisense (*Xba*I-*Sac*II for LAT1 only) fragments were isolated from these constructs and subcloned into the pTRE-Shuttle 2 vector containing an adenoviral expression cassette. Correct orientation of the LAT1 and 4F2 inserts was verified by DNA sequencing. PI-*Sce*I and I-*Ceu*I were used to excise the recombinant adenoviral expression cassette from these constructs for ligation into the pAdeno-X vector. *Pac*I released the recombinant LAT1 and 4F2 Adeno-X recombinant genomes for subsequent packaging, transfection and amplification in HEK cells. Lipofectamine Plus (Invitrogen, Carlsbad, CA) was used for transfection of the viral vector. Adenoviral stocks of β-galactosidase and TET regulatory virus (Adeno-X-TET-OFF) were from Clontech and amplified in HEK cells to levels of 1×10^{13} optical particle units (OPU) or greater and stored at −80°C. Viral titers were quantified in terms of OPU over several dilutions as directed by the Clontech Adeno-X user manual using a Genesys 5 spectrophotometer (Spectronic, Leeds, UK). Unless explicitly stated, all hepatic cells were co-infected with adenovirus containing the gene of interest together with the Adeno-X TET-Off regulatory virus. Optimal ratios were determined empirically as described in the Results section. For conditions in which exogenous expression was abrogated, doxycycline was added at Time 0 (0.0–10 μg/ml) to adenovirally infected cell cultures.

β-Galactosidase assay

Expression of β-galactosidase activity in adenovirally-infected cells was determined using a β-galactosidase Enzyme Assay System (Promega, Madison, WI). The β-galactosidase colorless substrate *O*-nitrophenol-β-d-galactopyranoside was added to extracts of lysed cells. Expression of the *O*-nitrophenol product was visualized as a yellow color quantified relative to a standard using a Bio-Kinetics EL-312 microplate reader (Bio-Tek Instruments Inc., Winooski, VT). *In situ* detection of β-galactosidase in cell cultures involved treating acetone fixed cells with potassium ferricyanide (5 mM), potassium ferrous cyanide (5 mM), magnesium chloride (2 mg/ml) and 5-bromo-4-chloro-3-indolyl β-d-galactopyranoside (X-gal) (1 mM in dimethylsulfoxide) in a PBS solution overnight at 37°C. The percentage of blue positive cells was quantitated by cell counts of several random fields at 20× magnification.

Transfection

The LAT1 plasmid expression vector pFLAG-CMV5arLAT1[19] was used for comparison with adenoviral infectivity. Normal AML12 murine hepatocytes were plated at 4×10^5 cells/well of 2-chamber slides (Fisher, Hampton, NH) 24 hr before transfection. For each chamber, 1.2 μg plasmid DNA, 6 μl Lipofectamine PLUS reagent (Invitrogen, Carlsbad, CA) and 3 μl Lipofectamine (Invitrogen) were combined and applied to cells for 3 hr as described previously.[19] Expression was assayed 72 hr later by indirect immunofluorescent staining for the FLAG epitope tag.

Hepatic cell cultures

The normal diploid rat hepatic epithelial line (WB-F344) (WB) originally isolated from an adult Fischer,[23] and a transformed, tumorigenic derivative (GP7TB) were kindly provided by Dr. W. Coleman (University of North Carolina, Chapel Hill).[18] Each cell line was maintained as described previously.[18,23] AML12 cells (a normal mouse hepatocyte line) were kindly provided by Dr. N. Fausto (Department of Pathology, University of Washington), and were maintained as described previously.[19]

Antibodies

FLAG fusion proteins were detected *in situ* on cell cultures with mouse anti-FLAG M2 monoclonal antibody (Sigma, St. Louis, MO) and FITC-conjugated secondary antibody (Sigma). FLAG fusion proteins were detected on Western blots with rabbit anti-FLAG IgG (Cayman Chemical, Ann Arbor, MI). LAT1/CD98lc was detected with affinity purified rabbit anti-peptide IgG (Serotec, Raleigh, NC) recognizing the N-terminal region.[19] Rabbit anti-peptide antisera to rat 4F2 as detected on Western blots was generously provided by Dr. S. Tate, (Weil Cornell Medical School, NY). Peroxidase-conjugated donkey anti-rabbit IgG (H & L) for Western blot detection was obtained from Jackson Laboratories (West Grove, PA).

Immunolocalization

Indirect immunofluorescent staining was carried out as described previously.[19] Fluorescent images were captured with a Nikon Eclipse E800 microscope, a Diagnostic Instruments Inc. RT Color Digital camera and associated SPOT software. Adobe Photoshop 7.0 was used to overlay images captured at different wavelengths (FITC for antigen detection and DAPI for nuclear stain).

Western blot analysis

Protein extracts of cultured cells were prepared by lysis of PBS rinsed monolayers in extraction buffer consisting of 150 mM NaCl, 50 mM TRIS (pH = 8.0) 1% Nonidet P-40 (Sigma, St. Louis, MO) and a protease inhibitor cocktail (Roche, Mannheim, Germany). Protein quantification was carried out using a BCA protein assay kit (Pierce, Rockford, IL) and albumin standard. For resolution of CD98 complexes under nondenaturing gel conditions, samples were prepared without mercaptoethanol. Proteins (10 μg/sample) were resolved by 10% SDS-PAGE and transferred to a nitrocellulose membrane using a semi-dry transfer cell. FLAG-tagged bacterial alkaline phosphatase (Sigma) provided a positive control on relevant Western blots.

RNA preparation and Northern blot analysis

Total RNA was isolated from cultured cells using the TRI reagent-RNA Isolation Reagent Method (TRI Reagent, RNA/DNA/Protein Isolation Reagent, Molecular Research Center Inc., Cincinnati, Ohio). Aliquots (10 μg) of total RNA were size fractionated on 1% agarose/formaldehyde gels as described previously.[7] After electrophoresis, gels were equilibrated in 1 mM ammonium acetate and RNA was transferred to nylon membranes. Blots were baked for 2 hr at 80°C. Hybridization with cDNA probes was carried out at 42°C in ULTRAhyb hybridization solution (Ambion, Austin, TX) sequentially to probes of interest. Random primed, P-32 labeled cDNA for TA1/LAT1 (as well as LAT2, 4F2/CD98 and GAPDH, data not shown) were as described previously.[18,19] After hybridization and washing, blots were exposed to X-ray film in the presence of intensifying screens or a Cyclone PhosphorImager (Model A431201) (Downers Grove, IL).

RT-PCR

Total RNAs were DNAase treated before random hexamer primed cDNA synthesis. Amplification of cDNA templates used LAT1 specific primers for endogenous (Forward 5′ GTGGCTGTGGATTTTGGGAAC 3; Reverse 5 ATTCACCTTGATGGGACGCTC 3) or exogenous [LAT1-FLAG fusion] (Forward 5′ GTGGCTGTGGATTTTGGGAAC 3; Reverse GTCTAGAAAGCTTCTACTTGTCGTC) sequences. 18S rDNA specific primers provided an internal normalization control. All PCR reactions were carried out in a GeneAmp PCR System 2700 Thermal Cycler (Applied Biosystems). Reactants were heated to 95°C for 5 min then cycled 35 times through 95°C for 30 sec; 55°C for 30 sec; 72°C for 1 min. A final incubation at 72°C for 10 min completed each amplification. PCR products were separated on a 3% agarose (TAE) gel and visualized by ethidium bromide staining. Digitized results were examined using NIH Image software to estimate changes in expression levels between LAT1-sense infected and uninfected controls.

Densitometry

Analysis of band intensities from Northern and Western blots and RT-PCR was carried out using a Versadoc Imaging System (model 3000) with associated Quantity One Software (Bio-Rad Laboratories, Hercules, CA). Band intensities were compared using adjusted intensity columns with local background subtracted. Analysis of PCR band densities also involved utilization of a Macintosh computer with an associated United States National Institutes of Health (NIH) Image software program version 1.6 (information is available online at http://rsb.info.nih.gov/nih-image).

Amino acid transport assays

The transport of tritium-labeled amino acids (NEN, Boston) by cell monolayers utilized a variation of the technique developed by Gazzola *et al.*[24] described by Kilberg[25] and used previously by our laboratory.[18] Statistical comparisons of transport categories utilized homoscedastic 2-tailed Student's *t*-tests. A *p*-value of 0.05 or less was considered statistically significant.

Growth assays

Cells were plated in 12-well culture plates at 5×10^5 cells/well on Day −1 then infected with 8×10^5 total OPU of the recombinant and regulatory viruses at a ratio of 3:1 on Day 0. Cells were harvested with trypsin-EDTA on Days 1–5 post-infection. Cell counts were carried out using a hemocytometer with trypan blue dye exclusion or a Guava Personal Cytometer (Guava Technologies Inc., Hayward, CA), where a minimum of 3,000 cells were collected per well.

Apoptosis and cell cycling

Cells were plated in 24-well culture plates at 5×10^5 cells/well on Day −1 then infected with 8×10^5 total OPU of the recombinant and regulatory viruses at a ratio of 3:1 on Day 0. Serum starvation was defined as removal of serum from medium for 48 hr between Days 0–2, at which time all wells were supplied with fresh medium. For each assay, a minimum of 3 wells were plated per category and 10,000 cells were collected per well using a Guava Personal Cytometer (Guava Technologies Inc., Hayward, CA). Levels of apoptosis were determined using the Guava Nexin kit as directed that allowed for demarcation of early apoptotic cells expressing Annexin V and late apoptotic cells that were additionally permeable to the 7-AAD dye (Guava Technologies Inc.). For cell cycling purposes, 5×10^5 cells in 0.5 ml were treated with 40 μl propidium iodide and quantified with a cytometer with associated Cell Quest software (Becton Dickinson, Bioscience Franklin Lakes, NJ) (2000 counts per tube). Analysis was carried out using ModFit LT software (Becton Dickinson, Bioscience Franklin Lakes, NJ). Statistical analyses were carried out on data from Days 3–5 post-infection using homoscedastic Student's *t*-tests.

Results

Optimization of adenoviral infection and expression

Initial experiments assessed the effectiveness of adenoviral expression and regulation in hepatic cells under short-term culture conditions. To this end, we utilized adenoviral-introduced β-galactosidase and adenoX-TET-Off as a control. This provided a means to assess viral driven expression both quantitatively and qualitatively with a gene not anticipated to affect cell growth or viability. Figure 2*a*,*b* shows a colorimetric assay for β-galactosidase expression at 3 days post-infection in AML12 cells demonstrating exogenous expression of >2 mU of β-galactosidase. As expected, inclusion of the tetracycline analog doxycycline (0.01–10 μg/ml) in virally infected cells effectively turned off β-galactosidase expression (Fig. 2*b*). Relative adenoviral expression and regulation was tested in normal murine and rat hepatocyte cell lines and the GP7TB hepatoma line with AdenoX-β-gal and an *in situ* X-gal staining (Fig. 2*c–e*). Under optimized conditions, virtually 100% of cells were infected and expressed viral product. Expression was TET-responsive in all cell types, as shown in Fig. 2*f–h*, where a >95% decrease in cells with β-galactosidase gene expression was observed in virally infected cultures treated with doxycycline. Thus, the same viral infection conditions were suitable for studies in all 3 hepatic cell lines of interest.

In other preliminary experiments, we assessed the effectiveness of adenoviral LAT1 expression in murine hepatic cells compared to plasmid transfection methods used previously[19] and optimized conditions of viral multiplicity of infection. Constructs for LAT1 contained an in-frame FLAG fusion protein that allowed detection

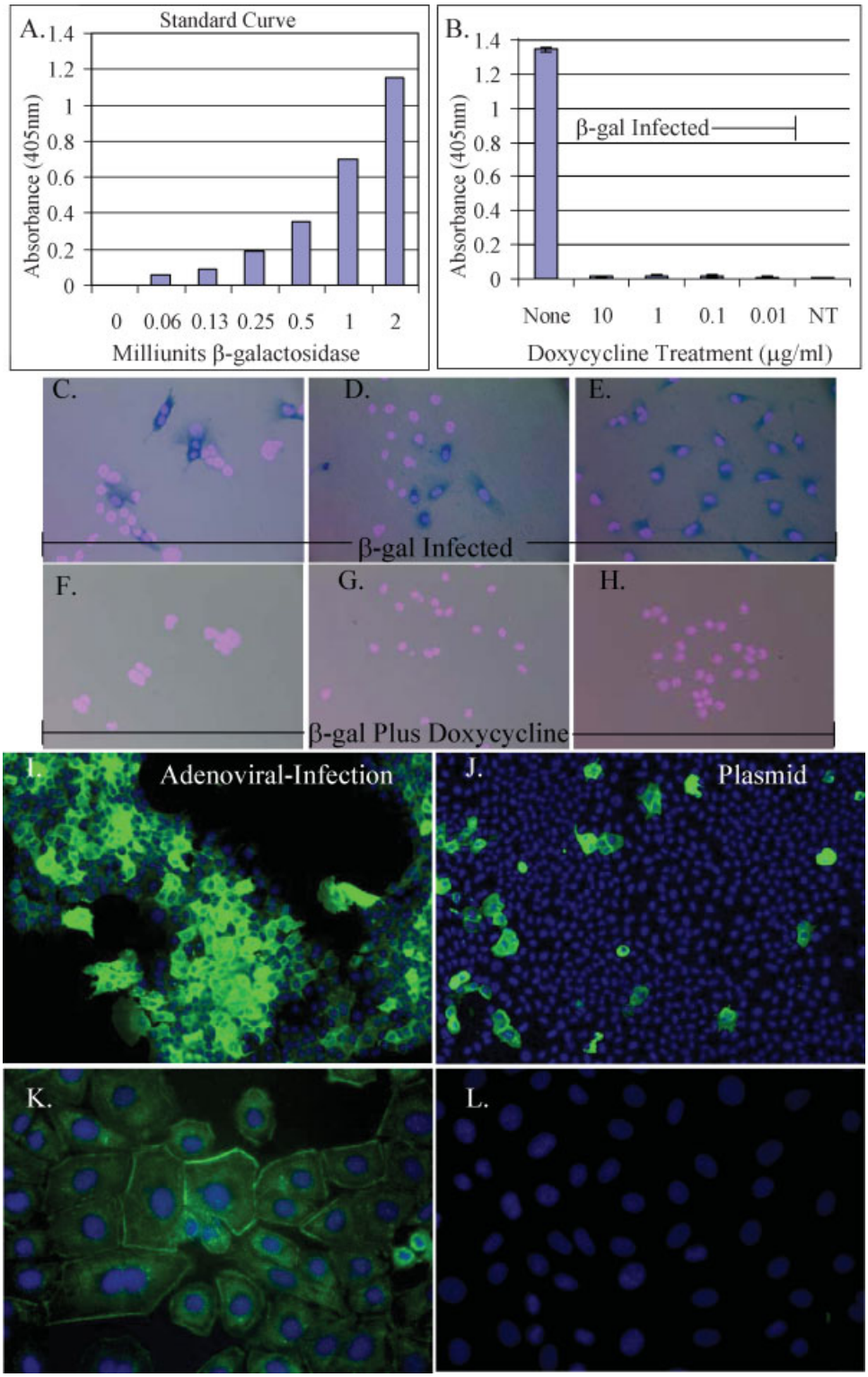

FIGURE 2 – Optimization of adenoviral infection and expression in hepatic cell lines 72 hr post-infection. (*a–h*) AdenoXT-β-gal driven expression. (*a*) β-galactosidase standard curve. (*b*) Colorimetric assay for β-galactosidase activity in extracts of virally infected murine AML12 hepatocytes without (none) or with doxycycline treatment (10, 1, 0.1, 0.01 μg/ml) to suppress expression *vs.* untreated control (NT). (*c–h*) *In situ* X-gal staining of rodent hepatic cell lines to demonstrate equivalent rates of cell infection and extinction of expression after doxycycline treatment. AdenoXT-β-gal-infected normal murine AML12 (*c,f*), rat WB (*d,g*), and transformed rat GP7TB (*e,h*). In the absence of doxycycline (*c–e*), dark blue β-galactosidase staining is visible in the cytoplasm of the majority of cells. Only nuclear counterstain is visible in virally infected cells treated with 1 μg/ml doxycycline (*f–h*). (*i,j*) Anti-FLAG immunofluorescent staining of AML12 cells expressing AdenoXT-LAT1-FLAG virus (*i*) *vs.* pCLAT1-FLAG plasmid (*j*) at 3-day time point showing greater percentage of FLAG positive virally infected cells. DAPI nuclear counterstain. Original magnification of cell culture photos = 200×. Cell surface staining for exogenous LAT1-FLAG is seen in rat WB hepatocytes in (*k*) *vs.* secondary antibody only (*l*). (*j–l*) Original magnification = 600×.

of the exogenous viral product using anti-FLAG antibodies either by immunofluorescence or Western blot. The percentage of infected cells was determined *in situ* as a ratio of FITC-stained cells to DAPI stained nuclei. A range of viral quantities and ratios of recombinant to regulatory virus were tested to determine optimal infection conditions. Figure 2*i* is a representative immunofluorescent image demonstrating expression of adenovirally-inserted LAT1-FLAG in normal, adult murine hepatic cells. Figure 2*j* shows corresponding FLAG expression in plasmid transfected murine hepatic cells. As expected, adenoviral infection was considerably more efficient than transfection, with up to 100% of virally infected cells expressing FLAG as tested through immunofluorescence. In comparison, plasmid transfection resulted in 9% FLAG positive cells with this cell type. Based on these optimization experiments, subsequent studies typically utilized ratios of 6×10^5 OPU/cell of recombinant virus and 2×10^5 OPU/cell for

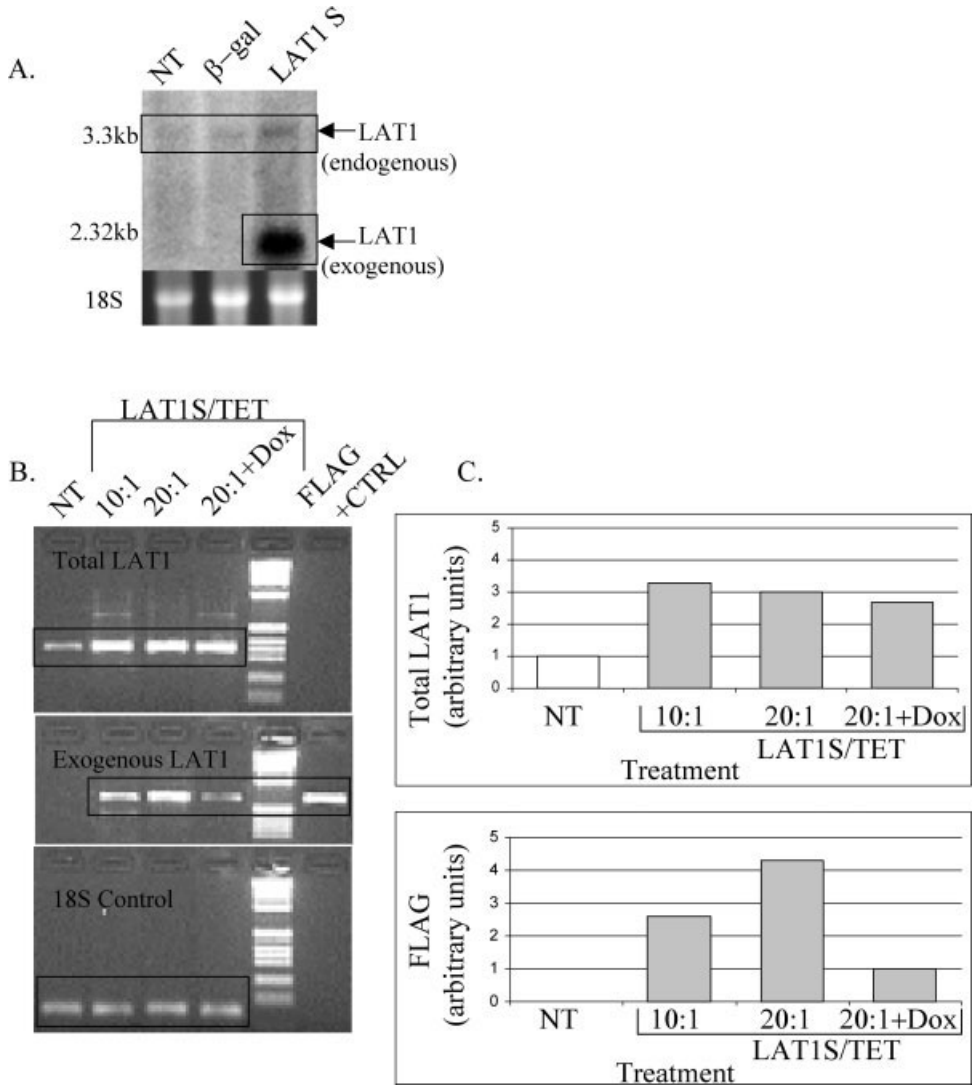

FIGURE 3 – LAT1 RNA levels are modulated in virally infected cells. (*a*) Phosphoimage of Northern blot showing steady state LAT1 levels in untreated, normal adult rat WB cells (NT) and those 3 days after infection with either AdenoXT-β-gal (β-gal) or AdenoXT-LAT1-FLAG. Band (3.3 kb) indicates endogenous rat LAT1 transcript, 2.3 kb band, exogenous LAT1. 18S rRNA control bands from corresponding lanes of ethidium bromide stained gel demonstrate equivalent loading. (*b*), Agarose gel of products from semi-quantitative RT-PCR. *Top*, Total LAT1. *Middle*, LAT1-FLAG. *Bottom*, 18S Control. *Lane 1*, NT (no treatment); LAT1-FLAG with 10:1 (*lane 2*) and 20:1 (*lane 3*) LAT1 to TET-Off viral ratios; *lane 4*, LAT1-FLAG with doxycycline treatment; *lane 5*, size marker ladder (M); *lane 6*, positive control for FLAG. (*c*) Densitometry of relative expression for Total LAT1 (*top*) and LAT1-FLAG (*bottom*) from gel shown in (*b*) (arbitrary units).

regulatory virus. Increasing this level 3-fold did not provide an infection advantage or result in additional functional responses. Immunofluorescence for the FLAG-tag was also used to examine localization of exogenously expressed LAT1. High power magnification of WB cells infected with LAT1-FLAG indicated definitive localization to the cellular membrane (Fig. 2*k*).

Expression and regulation of adenovirally-inserted LAT1 at the mRNA level

LAT1 expression and regulation at the mRNA level was determined using Northern blotting (Fig. 3*a*) and RT-PCR (Fig. 3*b*,*c*) to assess the quantitative impact of viral driven LAT1 expression in this system. Northern blots of WB cells 72 hr after infection of cells with LAT1 virus contained a viral-specific LAT1 transcript of approximately 2.2 kb in addition to the 3.4 kb endogenous transcript found in all rodent cells cultured under minimal media conditions (Fig. 3*a*). Semi-quantitative RT-PCR (Fig. 3*b*,*c*) showed that steady state LAT1 expression increased more than 3-fold in LAT1-sense infected cells (*lanes 2*, *3*) relative to uninfected controls (*lane 1*). Regulation of exogenous message was demonstrated in cells infected with LAT1 sense and treated with doxycycline (*lane 4*). In this case exogenous LAT1 expression was decreased 75% relative to cultures without the antibiotic regulator, demonstrating tight-control of exogenous expression.

Detection and regulation of adenovirally-expressed LAT1 protein

Western blotting was used to quantitate the expression and regulation of LAT1-FLAG and total LAT1 levels after LAT1-sense and antisense viral infection. A band of approximately 45 kDa corresponding to the size of LAT1 under reducing conditions was recognized by antibody to FLAG in extracts of normal adult rat hepatic cells infected with LAT1-FLAG containing adenovirus (Fig. 4*a*). This band was not present in extracts of cells infected with this virus together with doxycycline treatment (Fig. 4*a*). A smaller, inconsistent band was present in all lanes with the anti-FLAG antibody and seemed to be non-specific. In GP7TB cells infected with LAT1-antisense virus, a 3.2-fold difference was observed in the relative levels of the 45 kDa LAT1 band in antisense treated cells with and without doxycycline (Fig. 4*b*, *gel 1*). The second gel in Figure 4*b* shows replicate specimens. Viral constructs alone (β-galactosidase infected cells) are not responsible for significant alterations in LAT1 levels. These data demonstrate that viral driven changes in LAT1 RNA expression are reflected in corresponding quantitative changes at the protein level.

Association of adenovirally-expressed LAT1 with 4F2

After demonstrating that exogenous light chain was effectively produced and regulated, we asked whether the virally-expressed protein was able to interact with endogenous heavy chain to form CD98 heterodimers. Western blotting of protein extracts from vir-

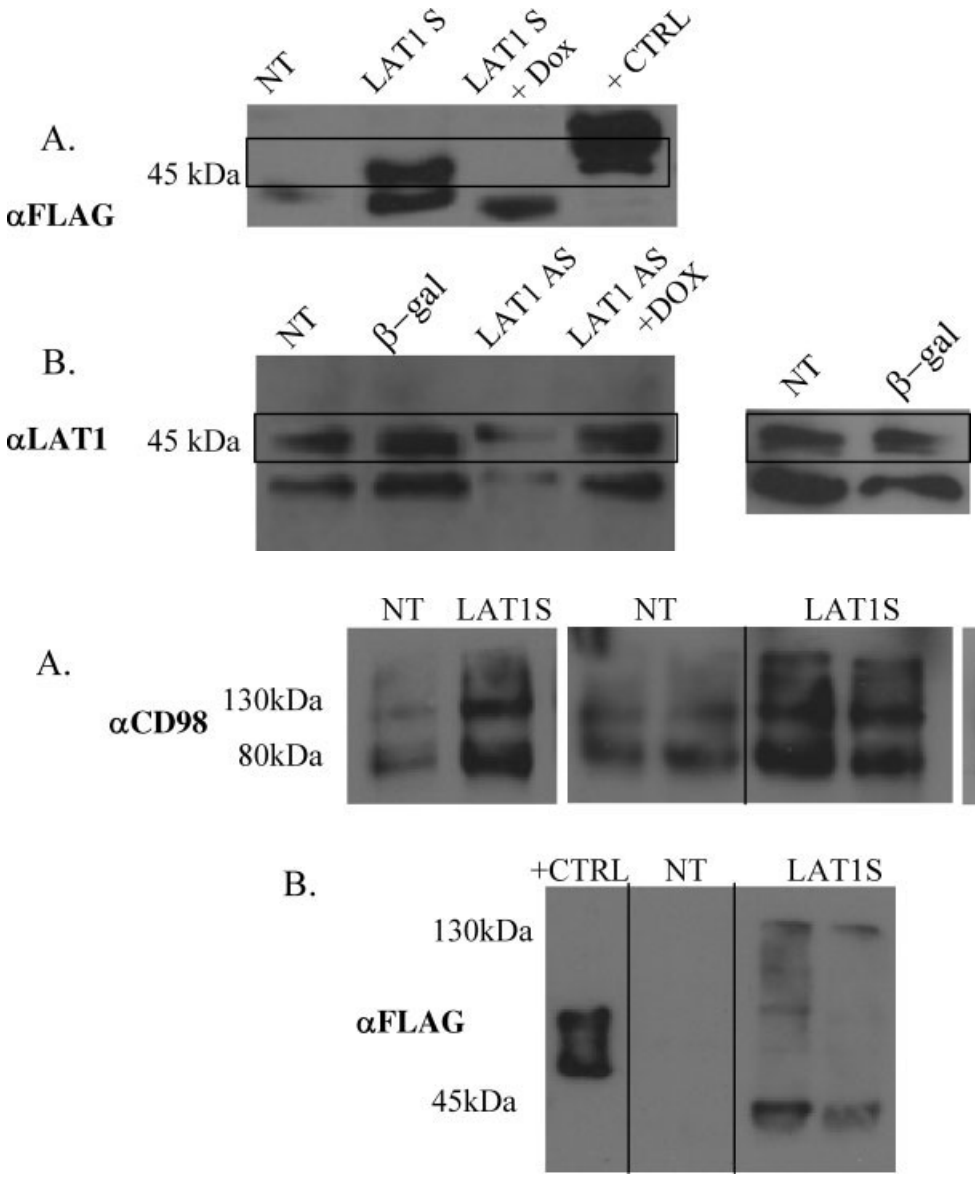

FIGURE 4 – Western blot expression and tetracycline-controlled regulation of adenoviral driven LAT1 in infected rat hepatic cells harvested 72 hr post-infection. (*a*) Anti-FLAG antibody, WB cells. From left, No Treatment, AdenoXT-LAT1-FLAG (sense), AdenoXT-LAT1-FLAG plus doxycycline, Positive Control FLAG protein. (*b*) Anti-LAT1 antibody, GP7TB cells. Two Westerns shown. From left, gel 1, No Treatment, AdenoXT-β-galactosidase, AdenoXT-1TAL (antisense), AdenoXT-1TAL (antisense) plus doxycycline. Gel 2, No Treatment, AdenoXT-β-galactosidase.

FIGURE 5 – Western blot of nonreducing gel demonstrating interaction of virally expressed LAT1 light chain with endogenous 4F2/CD98 heavy chain in WB cells. (*a*) Quadruplicate samples from 3 Western blots comparing 4F2 immunoreactive protein levels. NT, No Treatment; LAT1S, AdenoXT-LAT1-FLAG; β-gal, AdenoXT-β-galactosidase. (*b*) Anti-FLAG. From left, positive control for FLAG, No Treatment, replicate AdenoXT-LAT1-FLAG infected cells.

ally infected cells under non-reducing conditions with antibodies for the 4F2 heavy chain showed bands of 80 kDa (heavy chain alone) as well as 130 kDa, the expected size of the heterodimeric transporter. In WB cells there was an average 2.8-fold increase in level of the 130 kDa band in LAT1-sense infected cells as compared to untreated cells (first 3 examples, Fig. 5*a*). β-gal infection did not result in such increases (Fig. 4*a*, Western 3). Unexpectedly, we also observed a corresponding 2.4-fold increase in levels of the 80 kDa band in cultures expressing exogenous LAT1, suggesting that exogenous increases in light chain affected regulation of CD98 heavy chain as well. Anti-FLAG antibody confirmed that the 130 kDa band corresponding to CD98 heterodimer in the Adeno-X-LAT1 sense-infected cells contained virally expressed LAT1 light chain. The anti-FLAG antibody recognized a band at approximately 45 kDa, the expected size of the light chain (Fig. 5*b*) in addition to the band at 130 kDa. There was no corresponding anti-FLAG-reactive band in untreated cells (Fig. 5*b*). A similar increase in relative levels of total immunoreactive 4F2 was observed in independent protein extracts of LAT1-sense infected cells run under reducing conditions.

Effect of virally expressed LAT1 on leucine transport

Once it was established that a LAT1-4F2 complex was formed after adenoviral introduction of LAT1, we turned to functional assessment of leucine transport after LAT1-sense infection of normal mouse cells. Figure 6*a* shows the effect of exogenous LAT1 on System L (leucine) and non-System L (arginine) transport. Combined experiments with viral LAT1-sense infection demonstrated a significant increase in leucine transport relative to control mouse hepatic cells ($p < 0.001$). A 24.2% increase in leucine transport was observed 3 days post-infection. This increase was sensitive to the system L-selective inhibitor 2-amino-2-norbornane-carboxylic acid (BCH). As expected, no change was observed in transport of arginine, a non-system L substrate. No significant change in leucine transport was observed in LAT1-

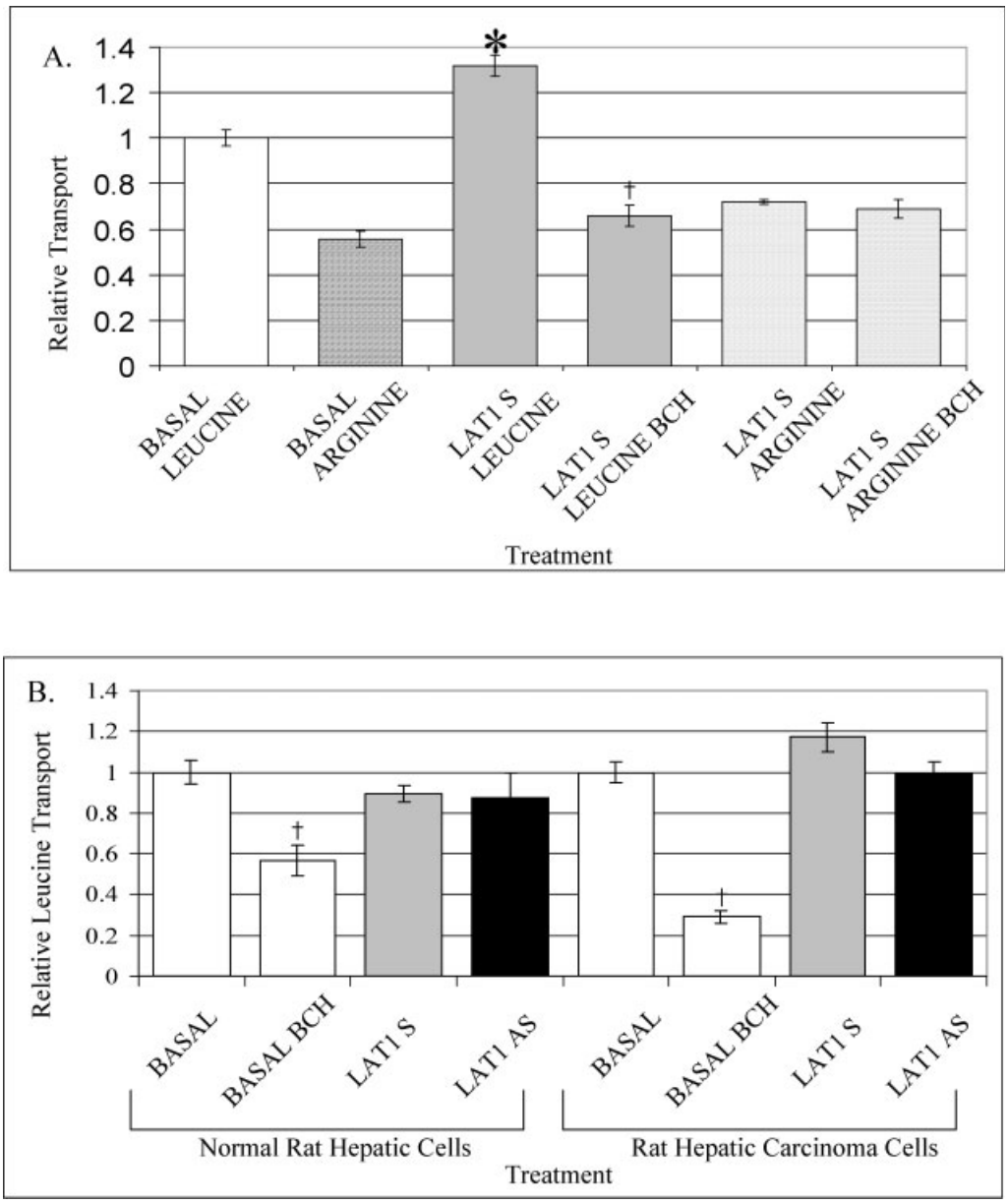

FIGURE 6 – Relative increase in leucine transport in AdenoXT-LAT1 infected murine but not rat hepatic cell lines. (*a*) Leucine (solid) and arginine (stippled) relative transport in normal AML12 cells. Basal, combined no infection treatment and AdenoXT-β-galactosidase (solid, white). LAT1S, AdenoXT-LAT1-FLAG (solid, gray) with or without BCH (10 mM). Combined data from 4 experiments with 3–6 replicates per condition, mean with SE. (*b*) Relative leucine transport in normal, WB rat hepatocytes (left) and GP7TB hepatoma cells (right). Basal, combined no infection treatment and AdenoXT-β-galactosidase (solid, white). LAT1S, AdenoXT-LAT1-FLAG (sense) infected cells (solid, gray). LAT1AS, AdenoXT-1TAL (antisense) infected cells (solid, black). Combined data from 3 experiments with 3–6 replicates per condition, mean with SE. *$p < 0.05$ *vs.* basal using homoscedastic 2-tailed Student's *t*-Test. †$p < 0.005$ *vs.* same treatment category without BCH.

infected rat hepatocytes or rat carcinoma cells (Fig. 6*b*), although a trend toward an increase in leucine transport was seen in carcinoma cells 3 days post-infection with LAT1-sense (Fig. 6*b*).

To assess whether viral titer was a factor affecting amino acid transport results, we examined whether altering the multiplicity of LAT1 infection or introducing 4F2 heavy chain alone (or in addition to LAT1) would further increase transport (Fig. 7*a*). Four LAT1 viral levels were tested (7.5×10^4, 1.5×10^5, 6×10^5, 2.4×10^6 OPU), and it was determined that 6×10^5 OPU of recombinant virus led to the greatest increase in leucine transport in murine cells (30% increase *vs.* basal, $p = 0.0058$). Adenoviral infection of the cells with exogenous 4F2 heavy chain alone increased leucine transport 20% ($p = 0.045$) *vs.* control cells, whereas a similar trend was observed with AdenoXLAT1 plus AdenoX-4F2 (16.2%) (Fig. 7*b*). There was no additive effect of coinfection with both heavy and light chain, suggesting perhaps that basal leucine transport levels may already be near maximal or that the viral product is not as effective a transporter as the endogenous complex.

Effects of LAT1-antisense on hepatocellular carcinoma cell number, viability and cell cycling

Because LAT1-antisense led to a decrease in mRNA and protein levels, we aimed to determine if alterations in cell viability, cell cycling, or cell numbers occurred after infection with LAT1 adenoviruses. Figure 8*a–c* shows GP7TB tumor cell number in

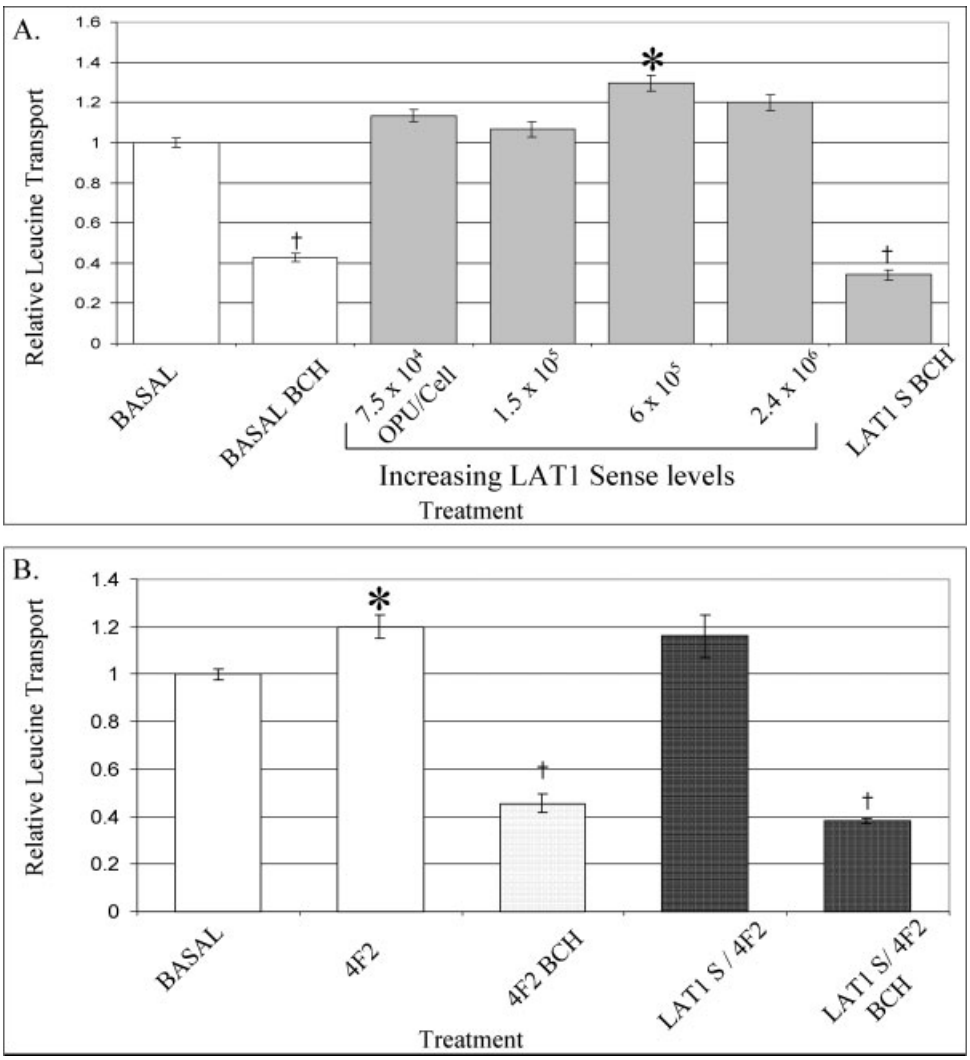

FIGURE 7 – Maximal leucine transport in AML12 cells is independent of increasing adenoviral LAT1 multiplicity of infection or exogenous 4F2 heavy chain. (*a*) From left, Basal, No Treatment and AdenoXT-β-galactosidase combined controls with or without BCH (solid, white); increasing multiplicity of infection with AdenoX-LAT1-FLAG [sense] (7.5×10^4, 1.5×10^5, 6×10^5, 2.4×10^6 OPU respectively) (solid, gray). (*b*) From left, Basal, No Treatment and AdenoXT-β-galactosidase combined controls (solid, white); 4F2, AdenoXT-4F2 [CD98 heavy chain] (6×10^5 OPU/cell) (stippled, white); LAT1S/4F2, AdenoX-LAT1-FLAG and AdenoXT-4F2 co-infected cells (stippled, gray) with or without BCH (100 mM). Mean with SE, 4–6 replicates per condition. $*p < 0.05$ *vs.* basal using homoscedastic 2-tailed Student's *t*-test. $\dagger p < 0.005$ *vs.* same treatment category without BCH.

LAT1S and LAT1AS infected cells, Days 3 (*a*), 4 (*b*), and 5 (*c*) post-infection. An increase in cell number was observed in LAT1S cultures at Day 3 ($p < 0.009$ *vs.* all categories), and a decrease in cell number at Day 4 in LAT1AS cultures ($p = 0.01$ *vs.* basal).

As an initial step toward elucidating the mechanisms altering cell numbers post-infection, analyses of cell cycling and apoptosis were carried out. Figure 8*d–e* shows cytometric data for cell viability (*d*), percentage of cells in the S-phase (*e*), and in G1 (F). All panels for Days 3 and 5 showed the same trends. LAT1-antisense decreased cell viability, decreased the percentage of cells in the S-phase of cycling, and increased the percentage of cells in G1. These differences were significant at the $p < 0.05$ level and independent of non-specific effects of viral (β-gal control) infection. LAT1-antisense expression thus results in decreased hepatocellular carcinoma cell growth.

Apoptosis was assessed in LAT1S or LAT1AS infected cells relative to a serum starved control to assess the relationship of apoptosis to changes in cell number. Early and late apoptotic states could be distinguished though cytometric analysis examining Annexin V expression and additional permeability to a 7-AAD dye. Apoptotic assays are shown in Figure 8*g–i*, which depicts cumulative data for Days 3–5 post-infection, showing non-apoptotic, early apoptotic, and late apoptotic percentages, respectively. An expected decrease in non-apoptotic cell percentage and an increase in apoptosis were seen in serum starved cells. There was a small but statistically significant increase in non-apoptotic cells in the LAT1S-treated category versus basal, and a significant decrease in late apoptosis in LAT1S treated-cells versus serum starved cells. The increase in carcinoma cell number after LAT1S-treatment, and the decrease cell number after LAT1AS-treatment seem to be due to a combination of factors. LAT1AS seems to have a net adverse effect on viability and cell cycling, whereas LAT1S may have a positive effect on cell survival although specific mechanisms are not yet known.

Discussion

Several laboratories including our own have reported increased LAT1 expression associated with neoplasia and postulated a direct growth or survival advantage in the tumor microenvironment. Despite the strong correlative association, it has not been clear whether up regulation of this system L amino acid transporter is a cause or a consequence of transformation. Such studies are complicated by the nearly ubiquitous expression of LAT1 by mammalian cells placed in culture and the paucity of *in vitro* model systems comparing normal epithelial cells with transformed derivatives. Though not envisioned as "oncogenic" in the traditional sense, selective transporter expression and regulation has the potential to contribute to the tumor cell's ability to survive and flourish in the metabolite-poor tumor microenvironment and collaborate with other genes in mediating well known "hallmarks of cancer."[26] Indeed, intake of substrates such as amino acids must be coordinated with processes of protein translation for the cell to properly adjust its growth rate to surrounding nutrient conditions,

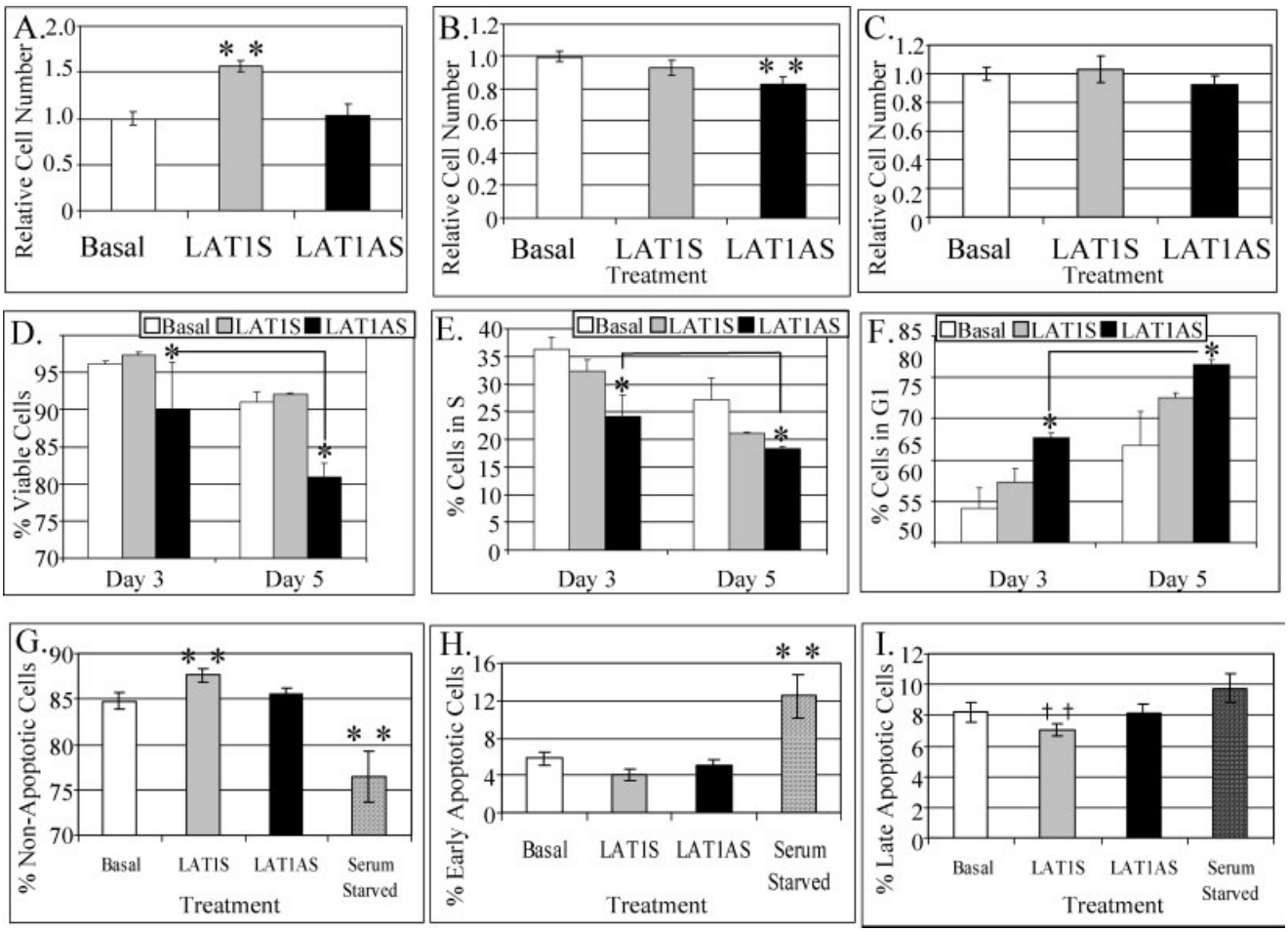

FIGURE 8 – Effects of LAT1-Sense and LAT1-antisense viral infection on GP7TB carcinoma cell number, viability, and cycling status. Basal, combined No Treatment, AdenoXT-β-galactosidase, and doxycycline controls (solid, white); LAT1S, AdenoXT-LAT1-FLAG (sense) infected cells (solid, gray); LAT1AS, AdenoXT-1TAL (antisense) infected cells (solid, black); Serum starved (striped). (*a–c*), relative viable cell number for Days 3–5 post-infection with LAT1S or LAT1AS, respectively (cumulative data from 6 assays, an average of 19 wells per category, 3,000 cells per well). (*d–f*) Results from cytometric assays on Days 3 and 5 post-infection, with 2–6 wells per category and 2,000 counts per well. (*d*) Viability. (*e*) Cells in S and (*f*) G1 phase of cell cycling for all harvest days. (*g–i*) Cumulative apoptosis data for Days 3–5 post-infection, showing non-apoptotic, early apoptotic and late apoptotic percentages, respectively (4 assays, 3–6 wells per category per assay, 10,000 cells collected per well). (*g*) Non-apoptotic cells. (*h*) Early apoptotic cells. (*I*) Late-apoptotic cells. Mean with SE (all panels). **p vs.* basal (*d–f*, Days 3 and 5 combined for statistics), ***p vs.* all categories, ‡*p vs.* serum starved, $p < 0.05$ using homoscedastic one-tailed Student's *t*-test.

and complex signaling pathways tightly control this balance in the normal cell.[27] Thus, alterations in expression, membrane targeting or stability of a high affinity transporter and obligate exchanger such as system L, with its wide substrate range, are well positioned for exploitation by the cancer cell. Of further interest is the report that overexpression of the 4F2 heavy chain, binding partner for the LAT1 light chain is sufficient for transformation in a mouse fibroblast model. Together 4F2 and any of several light chains, including LAT1, form the CD98 heterodimer and functional cell surface transporter.

To begin to examine these relationships, we utilized an adenoviral expression system and hepatic cell model system to assess the functional consequences of short term exogenous over expression and antisense expression of LAT1 relative to phenotypes associated with cancer. Adenoviral vectors offer the advantage of high-level exogenous gene expression in a wide variety of target cell types independent of proliferation status. When combined with tetracycline regulation, the system permits inducible modulation of expression both *in vitro* and *in vivo* with well matched control conditions to obviate potential artifacts of viral infection. Our adenoviral constructs were able to increase steady state levels of LAT1 RNA at least 3-fold over endogenous levels in normal rodent hepatocytes. Detection of the in-frame FLAG tag verified that the exogenous protein was expressed on the cell surface in the great majority of cells in an infected cell culture, and that expression was sensitive to the tetracycline analog doxycycline. To our knowledge, the only other viral system reported to manipulate system L in a mammalian cell utilized retroviral vectors in canine kidney cells and relative levels of exogenously driven expression were not reported.[28] Expression of the exogenous protein was doxycycline sensitive in that antibody to FLAG failed to stain the 45 kDa protein on Western blots of antibiotic treated infected cultures. At least a subset of adenovirally expressed LAT1 associated with endogenous 4F2 to form the CD98 complex as demonstrated by detection of a FLAG positive130 kDa complex on nondenaturing Western blots and co-reactivity with antibody to 4F2. Surprisingly, increased steady state levels of 4F2 and the CD98 complex were repeatedly observed on Western blots of hepatocyte cell cultures infected with LAT1 sense virus, implying some coordinate regulation or stabilization of the protein. Northern blot analysis of these cultures failed to show an increase in RNA levels for 4F2 under these conditions (data not shown), suggesting that the Western blot elevations might result from changes in protein turnover. Whether this might be due to the FLAG epitope tag is not known.

Clearly, the FLAG tag did not affect association with LAT1 or targeting to the plasma membrane.

Functional effects after increased LAT1 levels were cell-type specific and included changes in amino acid transport and cell number. Specifically, exogenous expression of LAT1 led to a significant increase in leucine transport in AML12 mouse hepatocytes relative to controls. Co-expression of 4F2 with LAT1 in AML12 cells at similar levels of multiplicity did not elevate transport over that observed with LAT1 alone, suggesting that endogenous levels of 4F2 were not limiting in these cells. In GP7TB cells, the increase in LAT1 was associated with an increase in total cell number at 3 days post-infection and a corresponding elevation of non-apoptotic cells. Although modest, these changes might be more robust in an *in vivo* model where amino acids are limiting.

The mechanisms by which exogenous LAT1 expression leads to the modest increases in cell number in GP7TB cells, and an increase in 4F2 heavy chain in WB cells are incompletely understood. The potential dependence of growth and survival alterations on the upregulation of 4F2 we observed after introduction of adenoviral LAT1 will require further study with appropriate, specialized reagents. Alterations in integrin signaling pathways in the absence of amino acid transport have not yet been examined in our system. It is well documented from the work of others that 4F2 interacts with integrins and affects integrin pathways, altering the activation state of Akt and RacGTPase, leading to changes in cellular morphology, susceptibility to apoptosis and contributing to tumorigenesis.[29] The examination of these pathways and their potential link to exogenous LAT1 expression will be of interest.

For reasons that are not clear, changes in transport in infected rat hepatic cell lines, either normal or transformed were not statistically significant compared to the mouse hepatic cells. The basis for the difference is not clear. LAT1 sequence is highly conserved between species such that LAT1 cRNA from multiple species is capable of driving transport in Xenopus oocytes. These cells were readily infected, demonstrated increased LAT1 RNA expression and were able to mediate functional adenovirally driven beta-galactosidase activity control at levels similar to the murine cell line. It is possible that an amino acid exchange mechanism in the rat cell lines might prevent accumulation of leucine as measured in the transport assay.

Effective downregulation of LAT1 expression was demonstrated in the adenovirally infected rat hepatic tumor cell line GP7TB. These are a tumorigenic derivative of the normal hepatic rat WB line and we have reported previously their high level endogenous LAT1 and 4F2 expression.[18] We utilized the antisense cDNA coding region in this vector system to have a matched control system that was TET-inducible. Western blot data verified a decrease in total LAT1 protein after short-term antisense expression and prompted assay of the associated phenotype. Despite up to 3-fold lower protein levels, no significant decrease in leucine transport was observed. No evidence for compensatory upregulation of other amino acid transporters was observed by Northern blot analysis (LAT2) and an initial Affymetrix rat expression microarray analysis (data not shown). Despite this result, cultures of tumor cells infected with antisense virus exhibited a significant decrease in viable cells over the experimental timeframe, which seems to result largely from a slow down in cell cycle progression through mechanisms yet to be fully elucidated. To address the possibility that the decrease in viability could be a consequence of non-specific viral infection, microarray gene expression analysis was carried out between LAT1-antisense infected GP7TB cells and controls. No increases were observed in 2′,5′-oligosynthetase 1 (Probe Set ID #1371152_a_at) or PKR-related proteins (Probe Set ID #1371899_at and #1387666_at) (data not shown).

We reported previously that LAT1 expression under conditions of low amino acid availability led to differential cell survival relative to controls in the AML12 cells. Our present data indicate that inhibition of LAT1 can independently diminish *in vitro* GP7TB cancer cell number by 18% over a 4-day period. A decrease in cell viability was observed for LAT1-antisense treated cells at Days 3 and 5 post-infection. In addition, a lower percentage of LAT1-antisense treated cells were found to be in the S-phase, and a higher percentage were in G1 at each time point. These alterations may be sufficient to account for the reduction in cell number that was observed. How this decrease in cell number may occur independent of an effect on amino acid transport is not known. Such growth related effects are similar to previous research in which 4F2 expression or function has been blocked,[21] as well as to studies blocking primary transporters for glutamine[30] and glucose.[31] Stable transfection of the human hepatoma cell line SK-Hep1 with an antisense RNA expression plasmid for the glutamine transporter ATB0/ASCT2 decreased mRNA levels 73% and resulted in decreased cell number at 48 hr.[30] Suppression of glucose transporter 1 (GLUT1) in the human gastric cancer cell line MKN45 resulted in a decreased number of cells in S-phase, at least partially due to an increase in p21 expression.[31] It remains to be determined whether modulation of other CD98-related functions such as mitogen stimulation or integrin activation are affected in cells with altered expression of LAT1. *In vivo* studies now in progress will mitigate the complication of induction of LAT1 expression in response to *in vitro* cell culture conditions and further assess the effects of this molecule on tumor growth and hepatic functions under more physiological conditions.

Acknowledgements

B. Storey was supported by a Brown University NIEHS Environmental Pathology Training Grant Postdoctoral Fellowship (T32ES007272). We extend thanks to N. Messier for assistance with the RT-PCR assay and to H.X. Leong for microarray gene analysis.

References

1. Sang J, Lim YP, Panzica M, Finch P, Thompson NL. TA1, a highly conserved oncofetal complementary DNA from rat hepatoma, encodes an integral membrane protein associated with liver development, carcinogenesis, and cell activation. Cancer Res 1995; 55:1152–9.
2. Tamai S, Musada H, Ishii Y, Suzuki S, Kanai Y, Endou H. Expression of L-type amino acid transporter 1 in a rat model of liver metastasis: positive correlation with tumor size. Cancer Detect Prev 2001; 25:439–45.
3. Ohkame H, Musada H, Ishii Y, Kanai Y. Expression of L-type amino acid transporter 1 (LAT1) and 4F2 heavy chain (4F2hc) in liver tumor lesions of rat models. J Surg Oncol 2001;78:265–72.
4. Yoon JH, Kim YB, Kim MS, Park JC, Kook JK, Jung HM, Kim SG, Yoo H, Ko YM, Lee SH, Kim BY, Chun HS, et al. Expression and functional characterization of the system L amino acid transporter in KB human oral epidermoid carcinoma cells. Cancer Lett 2004;205: 215–26.
5. Travers MT, Gow IF, Barber MC, Thompson J, Shennan DB. Indoleamine 2, 3-dioxygenase activity and L-tryptophan transport in human breast cancer cells. Biochem Biophys Acta 2004;1661: 106–12.
6. Kim DK, Kanai Y, Choi HW, Tangtrongsup S, Chairoungdua A, Babu E, Tachampa K, Anzai N, Iribe Y, Endou H. Characterization of the system L amino acid transporter in T24 human bladder carcinoma cells. Biochem Biophys Acta 2002;1565:112–22.
7. Wolf DA, Panzica MA, Wang S, Bassily NH, Thompson NL. Expression of a highly conserved oncofetal gene, TA1/E16, in human colon carcinoma and other primary cancers: homology to Schistosoma mansoni amino acid permease and Caenorhabditis elegans gene products. Cancer Res 1996;56:5012–22.

8. Verrey F, Closs EI, Wagner CA, Palacin M, Endou H, Kanai Y. CATs and HATs: the SLC7 family of amino acid transporters. Eur J Physiol 2004;447:532–42.
9. Verrey F, Jack DL, Paulsen IT, Saier MH Jr, Pfeiffer R. New glycoprotein-associated amino acid transporters. J Membrane Biol 1999; 172:181–92.
10. Mannion BA, Kolesnikova TV, Lin SH, Wang S, Thompson NL, Hemler ME. The light chain of CD98 is identified as E16/TA1 protein. J Biol Chem 1998;273:33127–9.
11. Meier C, Ristic Z, Klauser S, Verrey F. Activation of system L heterodimeric amino acid exchangers by intracellular substrates. EMBO J 2002;21:580–9.
12. Yanagida O, Kanai Y, Chairoungdua A, Kim DK, Segawa H, Nii T, Cha SH, Matsuo H, Fukushima J, Fukasawa J, Tani Y, Taktani Y, et al. Human L-type amino acid transporter 1 (LAT1): characterization of function and expression in tumor cell lines. Biochem Biophys Acta 2001;1514:291–302.
13. Broer A, Wagner CA, Lang F, Broer S. The heterodimeric amino acid transporter 4F2hc/y+LAT2 mediates arginine efflux in exchange with glutamine. Biochem J 2000;349:787–95.
14. Cho JY, Skubitz KM, Katz DR, Chain BM. CD98-dependent homotypic aggregation is associated with translocation of protein kinase C delta and activation of mitogen-activated protein kinases. Exp Cell Res 2002;286:1–11.
15. Kudo Y, Boyd CAR, Millo J, Sargent IL, Redman CWG. Manipulation of CD98 expression affects both trophoblast cell fusion and amino acid transport activity during syncytialization of human placental BeWo cells. J Physiol 2003;550:3–9.
16. Rintoul RC, Buttery RC, Mackinnon AC, Wong WS, Mosher D, Haslett C, Sethi T. Cross-linking CD98 promotes integrin-like signaling and anchorage-independent growth. Mol Biol Cell 2002;13: 2841–52.
17. Hara K, Kudoh H, Enomoto T, Hashimoto Y, Masuko T. Enhanced tumorigenicity caused by truncation of the extracellular domain of GP125/CD98 heavy chain. Oncogene 2000;19:6209–15.
18. Campbell WA, Sah DE, Medina MM, Albina JE, Coleman WB, Thompson NL. TA1/LAT-1/CD98 light chain and system L activity, but not 4F2/CD98 heavy chain, respond to arginine availability in rat hepatic cells. Loss of response in tumor cells. J Biol Chem 2000;275: 5347–54.
19. Campbell WA, Thompson NL. Overexpression of LAT1/CD98 light chain is sufficient to increase system L-amino acid transport activity in mouse hepatocytes but not fibroblasts. J Biol Chem 2001;276: 16877–84.
20. Shishido T, Uno S, Kamohara M, Tsuneoka-Suzuki T, Hashimoto Y, Enomoto T, Masuko T. Transformation of BALB3T3 cells caused by over-expression of rat CD98 heavy chain (HC) requires its association with light chain: mis-sense mutation in a cysteine residue of CD98HC eliminates its transforming activity. Int J Cancer 2000;87:311–6.
21. Papetti M, Herman IM. Controlling tumor-derived and vascular endothelial cell growth: role of the 4F2 cell surface antigen. Am J Pathol 2001;159:165–77.
22. Yagita H, Masuko T, Hashimoto Y. Inhibition of tumor cell growth in vitro by murine monoclonal antibodies that recognize a proliferation-associated cell surface antigen system in rats and humans. Cancer Res 1986;46:1478–84.
23. Tsao MS, Smith JD, Nelson KG, Grisham JW. A diploid epithelial cell line from normal adult rat liver with phenotypic properties of 'oval' cells. Exp Cell Res 1984;154:38–52.
24. Gazzola GC, Dall Asta V, Franchi-Gazzola R, White MF. The cluster-tray method for rapid measurement of solute fluxes in adherent cultured cells. Anal Biochem 1981;115:368–74.
25. Kilberg MS. Measurement of amino acid transport by hepatocytes in suspension or monolayer culture. Methods Enzymol 1989;173: 564–75.
26. Hanahan D, Weinberg RA. The hallmarks of cancer. Cell 2000;100: 57–70.
27. Schmelzle T, Hall MN. TOR, a central controller of cell growth. Cell 2000;103:253–62.
28. Bauch C, Forster N, Loffing-Cueini D, Summa V, Verrey F. Functional cooperation of epithelial heteromeric amino acid transporters expressed in madin-darby canine kidney cells. J Biol Chem 2003; 278:1316–22.
29. Feral CC, Nishiya N, Fenczik CA, Stuhlmann H, Slepak M, Ginsberg MH. CD98hc (SLC3A2) mediates integrin signaling. PNAS 2005; 102:355–60.
30. Fuchs BC, Perez C, Suetterlin JE, Chaudhry SB, Bode BP. Inducible antisense RNA targeting amino acid transporter ATB0/ASCT2 elicits apoptosis in human hepatoma cells. Am J Physiol 2004;286:G467–8.
31. Noguchi Y, Saito A, Miyagi Y, Yamanaka S, Marat D, Doi C, Yoshikawa T, Tsuburaya A, Ito T, Satoh S. Suppression of facilitative glucose transporter 1 mRNA can suppress tumor growth. Cancer Lett. 2000;154:175–82.